Construction and Building Materials 486 (2025) 141972

Contents lists available at ScienceDirect

Construction and Building Materials

journal homepage: www.elsevier.com/locate/conbuildmat

Investigation into the healing properties of bituminous mastics with bio-oil and steel slag

Marina Cabette [a], Rui Micaelo [b,*], Jorge Pais [c]

[a] ISISE, Dept. of Civil Engineering, University of Minho, Guimarães, Portugal
[b] CERIS, Dept. of Civil Engineering, NOVA School of Science and Technology, Caparica, Portugal
[c] ISISE, Dept. of Civil Engineering, University of Minho, Guimarães, Portugal

ARTICLE INFO

Keywords:
Bituminous mastic
Bio-oil
Steel-slag
Fatigue testing
Healing

ABSTRACT

This study evaluated the healing properties of bituminous mastics containing bio-oil derived from biodiesel production and steel slag. Various healing indices related to the complex shear modulus, fatigue life and load-induced damage were evaluated using time sweep tests with rest periods. The bio-oil showed a great capacity to reverse the ageing effects in bitumen, and the fatigue resistance of mastics improved with the bio-oil content. The impact of oxidative ageing and filler type on the stiffness properties and fatigue resistance varied depending on the mastic composition. The mastics were unable to fully recover their initial state under the resting conditions applied, and healing capacity decreased with each successive loading period. The most significant effect of the rest period was observed in the healing index related to the complex shear modulus, suggesting that this healing index accounts for a large proportion of the non-damaging effects associated with cyclic loading. The healing capacity was generally higher for the mastics containing bio-oil, although the degree of improvement varied depending on the mastic composition and the specific healing index considered. The influence of filler type on healing capacity was relatively minor, however, steel slag powder was shown to be a viable alternative to limestone filler.

1. Introduction

Research into the healing capabilities of bituminous materials is pivotal to enhancing the durability and resilience of bituminous pavements. The healing process relies on the ability of bitumen to flow and redistribute under specific thermal and stress conditions to close microcracks. The main healing mechanisms are viscoelastic flow, diffusion, and recrystallisation [1–3]. Several internal and external factors influence healing. The chemical, rheological and mechanical properties of bituminous materials are important internal factors. Some relevant external factors are the temperature and the time between loading cycles [4,5]. Hence, temperature is critical to healing as bitumen viscosity decreases with increasing temperature, facilitating healing. Changes in the chemical composition due to ageing can also impact the healing capacity, with higher molecular weight compounds reducing viscosity. Based on these healing mechanisms, various strategies to enhance this process, such as reducing viscosity, are being explored [6,7]. The reduction of viscosity can be achieved through various means, such as by increasing the temperature for a short period of time using induction and microwave heating [8,9] or by adding encapsulated softening agents [10]. Nevertheless, these approaches are still under development and the industrial application is limited to field trials [11,12].

Therefore, it is clear that the viscosity of the bitumen, and consequently of the mastic, has a huge importance in the self-healing capabilities through its flow, diffusion and recrystallisation capacities. So, for better understanding how the reduction of viscosity with softening agents contributes to the durability of bituminous materials, this study investigates the healing properties of bituminous mastics, which include softening agents like bio-oil and fillers such as industrial waste materials. Bituminous mastic, composed of bitumen and finer aggregate particles, significantly affects the overall behaviour of bituminous mixtures. The interaction between bitumen and filler particles can alter the flow and redistribution of bitumen during the healing process. In addition, the filler's surface chemistry, including its surface area, particle size, and texture, is crucial to understanding how it influences bitumen's behaviour and the healing efficiency [13–17].

The literature [15] suggests that around each solid filler particle,

* Corresponding author.
E-mail addresses: marinacabette@gmail.com (M. Cabette), ruilbm@fct.unl.pt (R. Micaelo), jpais@civil.uminho.pt (J. Pais).

https://doi.org/10.1016/j.conbuildmat.2025.141972
Received 23 October 2024; Received in revised form 20 May 2025; Accepted 24 May 2025
Available online 29 May 2025

there is a volume of bitumen whose behaviour is altered by this interaction. Closer to the filler particle, the bitumen is completely immobilised (fixed) due to the adsorption of specific bitumen compounds (asphaltenes and resins [16]) on the surface of the filler particle through electrostatic forces, hydrogen bonding and van der Waals interactions [17]. In contrast, the bitumen is only partially affected further away from the solid particle because the interaction powder decreases with the distance from the particle. Fillers of different origins, natural and industrial, have different surface chemistry characteristics, corresponding to different electrokinetic properties and active sites to adsorb the most polar compounds of bitumen. However, according to the study conducted by Clopotel *et al.* [13], the most critical factor in the amount of bitumen compounds adsorbed is the surface area of the filler and not the chemical composition. Filler surface area varies greatly with the particle size, shape and surface texture. Nevertheless, the surface chemistry of the filler is still vital in determining the physical bond strength, particularly under the influence of water, because some bitumen functional groups, such as carboxylic acid and phenolic, react with the filler components present on the surface to form water-soluble salts that weaken the interface over time or, conversely, water-insoluble salts that strengthen the interface [17].

Due to obvious economic and environmental benefits, waste materials have been investigated as a substitute for mineral fillers. Among the various wastes commonly available, steel slag is a residue from the steel production process that can replace natural mineral aggregates in the construction industry due to its physical and chemical properties [18,19]. Steel slag is a hard, high-strength granular material rich in different calcium compounds (*e.g.* calcium oxide, dicalcium silicate, etc.) [20]. In Europe, steel slag is mostly reused in road construction (nearly 70 % [21]). Regarding its use in bituminous mixtures, most studies in the literature analysed the replacement of coarse aggregates. As described by Pasetto *et al.* [21], the performance is generally better in bituminous mixtures containing steel slag because the high angularity and stiffness properties of the steel slag particles result in more significant particle interlocking, and the rough texture combined with the excellent bitumen-aggregate (chemical) affinity enhances the adhesion and cohesion properties of the mixture. However, the optimum bitumen content in mixtures increases due to the particles' porous surface. In the literature are also found studies that investigated the use of steel slag in the filler fraction of bituminous mixtures. Meng *et al.* [22] evaluated the performance of bituminous mastics incorporating steel slag and recycled crumb rubber, analysing the complex shear modulus, multi-stress creep recovery properties, and zero shear viscosity, and concluded that the steel slag powder improves the mechanical properties of the mastics, especially in the high-temperature service range. Tao *et al.* [23] investigated the replacement of limestone filler by steel slag, and the results obtained showed greater deformation resistance but slightly lower low-temperature cracking resistance. Hence, the authors recommended restricting the replacement of limestone filler by steel slag to 75 % of the filler content. Zhang *et al.* [24] investigated the fatigue properties of the mastics with steel slag filler using time sweep tests. They found that substituting limestone filler with steel slag filler in the mastic improved the fatigue resistance. Compared to limestone mastic, the complex shear modulus of steel slag mastic showed an increase of 84.9 %, 118.0 %, and 256.1 % when using 30 %, 50 % and 100 % steel slag.

Furthermore, adding steel slag filler to the mastic enhances its thermal properties. Li *et al.* [9] found that steel slag filler-based mastics exhibited higher heating rates under microwave irradiation than those with limestone filler, attributed to the slag's higher relative complex permittivity and porous structure. They then applied a fatigue–healing–fatigue test, where specimens were fatigued until their complex modulus dropped to 50 % of the initial value, followed by microwave heating for healing. After cooling, the samples underwent a second fatigue test. The results showed that the initial complex shear modulus of the mastic with steel slag filler was restored to approximately 76 %, and the number of cycles to failure was 14 % greater than that of the mastic with limestone filler, indicating a significant extension of the fatigue life after healing. Dai *et al.* [25] evaluated the induction healing using a bending beam fatigue test. The healing results of the specimens showed that after nine fracture-healing cycles, the mastic specimens with steel slag had a recovered strength of 160–209 %. Grossegger *et al.* [26] used the three-point bending test to evaluate the heat-induced healing properties. The healing results of the specimens showed an average healing rate of 75 % after one month at ambient temperature.

In addition to steel slag, bio-oils have shown potential as effective bitumen additives to reverse oxidative ageing and promoting healing. Bio-oils can improve the fatigue and thermal cracking resistance of bitumen by reducing fatigue damage and decreasing the ratio of residual stress to relaxation time [27,28]. Also, they can contribute to the softening of aged bitumen, restoring the coefficient of thermal expansion and increasing the ductility of the binder [29–31]. Lei *et al.* [32] examined the effect of bio-oil on the shear properties, high-temperature rheological behaviour, and low-temperature flexibility of mastics. They found that the shear strength of bituminous mastics, with or without bio-oil, increases with the filler-to-binder ratio. Moreover, the incorporation of bio-oil enhances the high-temperature stability of the mastics, resulting in greater resistance to permanent deformation compared to neat bituminous mastics, particularly within the filler-to-binder ratio range of 1.0–1.4. In a previous study [5], it was observed that a bio-oil, derived from the biodiesel production process, can increase the restoration of the bitumen during rest periods between cycling loading. For every 1 % increase in bio-oil, the average increase in healing index varied between 1.1 % and 3.3 % depending on the bitumen ageing level.

In summary, while previous research has shown that bio-oils can effectively soften bitumen and that steel slag may serve as a viable replacement for natural aggregates, their combined impact on the healing behaviour of bituminous mastics remains underexplored.

2. Objectives and scope

This study aims to address the gap in understanding the combined effects of bio-oil and steel slag on the mechanical and healing properties of bituminous mastics without the use of external heating methods. The objective was to evaluate the healing properties of bituminous mastics modified with bio-oil derived from biodiesel production, focusing on the role of steel slag as a substitute for limestone filler.

The study analysed the fatigue behaviour and healing ability of mastics with varying bio-oil content, different fillers, and at different ageing levels. Fatigue behaviour was characterized using the Linear Amplitude Sweep (LAS) test and the Time Sweep Test with Rest Periods (TST-RP). Several healing indices related to complex shear modulus recovery, fatigue life, and loading-induced damage were assessed. Additionally, the experimental plan included the characterization of the geometric and chemical properties of the fillers, as well as the consistency and rheological behaviour of the mastics.

3. Materials and methods

3.1. Materials

The bitumen used in this study is a 35/50 penetration grade bitumen, a semi-hard class bitumen with the properties shown in Table 1. This bitumen was adopted because is a commonly used bitumen in south

Table 1
Properties of 35/50 penetration grade bitumen.

Property	Test method	Value
Penetration at 25°C (0.1 mm)	EN 1426 [35]	37
Softening point (°C)	EN 1427 [36]	53
Dynamic viscosity at 150°C (Pa.s)	EN 13302 [37]	0.68

European countries, currently the most used in Portugal. The bitumen was studied under three different oxidative ageing conditions: unaged (U), short-term aged (R), and long-term aged (P). Short-term ageing was simulated using the Rolling Thin Film Oven (RTFOT) protocol defined in test standard EN 12607–1 [33], while long-term ageing was simulated using the Pressure Ageing Vessel (PAV) protocol defined in test standard EN 14769 [34]. The long-term aged bitumen sample was subjected to RTFOT and PAV procedures.

A rejuvenating agent (bio-oil) is used to reverse the oxidative ageing in bitumen and to promote self-healing mechanisms. The bio-oil (BO) studied is a mixture (50/50 by weight) of the residue from the biodiesel production process, which contains a variable range of organic compounds with lower volatility than those found in biodiesel and fatty acid methyl ester. The bio-oil composition can vary depending on the feedstock used and the distillation process. The BO has a strong thermal stability in the range of temperatures used to produce bituminous mixtures. The thermogravimetric analysis of BO showed a weight loss of only 0.5 % at 135 ºC and 4.5 % at 175 ºC [38].

Limestone powder and steel slag powder were used in bituminous mastics. Table 2 lists the main properties of these fillers. The steel slag filler is the fraction of the material that passes the 0.125 mm opening sieve after grinding in the laboratory. The fillers were dried in a ventilated oven at 150 ºC for 24 h and stored in a desiccator before use.

3.2. Experimental methods

3.2.1. Preparation of bituminous mastics

This study produced and tested twenty-four bituminous mastics, combining four bitumens, three ageing states and two fillers. The filler content in mastics was 30 % by volume, an intermediate value for conventional dense bituminous mixtures [42]. The bitumen was modified by 1 %, 2 %, and 3 % by the weight of the bio-oil (proportions of the final mix). The bio-oil was blended with the bitumen previously conditioned to the three different ageing states (unaged, short-term and long-term) using a low-shear mixer at 200 rpm for 5 minutes and at a temperature of 135°C. The fillers are the limestone filler (L) and a mixture of limestone and steel slag filler (S) (50/50 by volume). The steel slag filler alone was not tested due to the risk of reducing the workability of the bituminous mastic. Thus, in [23], the authors recommended restricting the replacement of limestone filler by steel slag to 75 % of the filler content. For this reason, a more conservative value of 50 % of steel slag was adopted in this study.

To prepare the mastic samples, the filler and bitumen were first heated to 150 ºC for one hour, and then the filler was added to the bitumen by hand with mechanical stirring at 400 rpm. The mixing process was completed in 30 min. These conditions were based on previous work [42], which demonstrated their effectiveness in producing homogeneous mastic mixtures with various types of bitumen and fillers.

To facilitate the identification of each mastic sample and its results and subsequent discussions, the material ID was defined in the paper by the acronym formed by the filler type (L or S) and the bitumen ageing state (U, S and P). The bitumen's bio-oil percentage is added at the end of the acronym. For example, "LP2" refers to the mastic with limestone filler and the long-term aged bitumen modified with 2 % bio-oil.

Table 2
Properties of fillers.

Property	Density (g/cm^3)	Voids (%)	Particle gradation EN 933 [39]		
	ASTM 188 [40]	EN 1097–4 [41]	0.500 mm	0.125 mm	0.063 mm
Limestone	2.68	21	100	93	75
Steel slag	3.63	24	100	100	62

3.3. Scanning electron microscopy and energy-dispersive X-ray spectroscopy tests

The Scanning Electron Microscopy (SEM) and Energy-Dispersive X-ray Spectroscopy (EDS) techniques were used to characterise the geometric and chemical properties of the fillers studied. The SEM is a microscopy technique that produces high-resolution images of a sample by scanning it with a focused beam of electrons. SEM can provide detailed information about the surface morphology and texture of materials. Morphological analyses were performed in an ultra-high resolution Field Emission Gun Scanning Electron Microscopy (FEG-SEM), NOVA 200 Nano SEM. Topographic images were obtained using a secondary electron detector at an acceleration voltage of 10 kV. EDS is an analytical technique commonly used in conjunction with SEM to determine the elemental composition of a sample. Chemical analyses of the samples were performed using the energy dispersive spectroscopy technique and an EDAX Si(Li) detector at an acceleration voltage of 15 kV. Before morphological analysis, the samples were coated with a thin film (25 nm) of Au-Pd (80–20 wt%) in a high-resolution sputter coater, 208HR Cressington Company, coupled to an MTM-20 Cressington high-resolution thickness controller.

3.4. Consistency tests and rheological characterisation

The consistency of the different mastics was evaluated at intermediate temperatures by the needle penetration test according to European standard EN 1426 [35] and at higher temperatures by determining the softening point using the ring and ball test according to European standard EN 1427 [36].

Additionally, a frequency sweep test (first part of the AASHTO-TP 101–14[43] procedure) (0.2–30 Hz) at a low strain amplitude (γ = 0.1 %) was carried out using a dynamic shear rheometer to characterise the linear viscoelastic rheological behaviour at an intermediate temperature (20 ºC).

3.5. Fatigue behaviour

3.5.1. Linear amplitude sweep (LAS) test

The LAS test is an accelerated test method used to evaluate the fatigue resistance of bituminous materials, excluding any recovery and healing mechanisms that occur during the resting period. This test provides a complementary evaluation to the time sweep test with rest periods of the fatigue resistance of bituminous mastics.

This study applied the LAS test protocol and analysis procedure, described in AASHTO-TP 101–14 [43], to the mastics studied. In summary, the test was performed at an intermediate temperature of 20 ºC, using a parallel plate setup with disc-shaped specimens of 8 mm diameter and 2 mm height. This test involves oscillatory load cycles with progressively increasing amplitudes. The strain amplitude (γ) starts at 0.1 %, followed by increments from 1 % to 30 %, with a consistent increase of 1 % every 10 seconds of loading (constant loading frequency of 10 Hz). The test results are analysed based on the Viscoelastic Continuum Damage (VECD) theory [44]. In AASHTO-TP 101–14 [43], the viscoelastic stiffness properties (modulus and phase angle) are determined every cycle from the strain and load values, and the material integrity C at cycle i is obtained as:

$$C_i = \frac{|G^*|_i}{|G^*|_{initial}} \tag{1}$$

where, $|G^*|_i$ is the complex shear modulus at cycle i and $|G^*|_{initial}$ is the initial complex shear modulus describing the undamaged condition of the material. The damage intensity at time t, related to the number of cycles N and the frequency f, is also determined as:

$$S_t = \sum_{i=1}^{N} \left[\pi \times \gamma^2 \times (C_{i-1} - C_i)\right]^{\frac{\alpha}{1+\alpha}} \times (t_i - t_{i-1})^{\frac{1}{1+\alpha}} \quad (2)$$

where α is the inverse of the maximum slope of the relaxation modulus-time curve determined for each specimen before the fatigue test using the test protocol described in section 3.2.3. Then, the $C - S_t$ results along the test are fitted with a power law model, as:

$$C = C_0 - C_1 \times S_t^{C_2} \quad (3)$$

To determine the fatigue law, the failure point of the individual test result is defined when the maximum shear stress is registered, and the damage intensity at the failure point (S_f) is calculated with fitted model (Eq. (3)). The estimated number of cycles to failure (N_f) at the defined strain amplitude γ is determined as:

$$N_f = \frac{f \times S_f^{1+(1-C_2)\times\alpha}}{(1+(1-C_2)\times\alpha)(\pi \times C_1 \times C_2)^{\alpha}} \times \gamma^{2\alpha} \quad (4)$$

where, f is the loading frequency. The mathematical deduction of Eq. (4) from the implementation of the VECD to the analysis of bitumen cyclic tests can be found in [44].

3.6. Time sweep test with rest periods (TST-RP)

The fatigue resistance of bituminous mastics, considering the positive contribution of viscoelastic and healing mechanisms during the rest periods, was assessed using time sweep tests in a strain-controlled mode, following a procedure similar to that described in [2,45,46]. The protocol corresponds to a time sweep test with rest periods. In the analysis of the test results, the overall change in mechanical properties during the rest period is used as an indicator of healing.

The basic procedure consists of a series of loading and rest periods. During the loading phase (indexed as $i = 1, 2, \ldots$), the test is stopped when the complex shear modulus ($|G^*|$) falls to 50 % of its initial value (representing an undamaged state). The duration of the rest period (indexed as $j = 1, 2, \ldots$) remains constant (see Fig. 1). The tests were conducted at a temperature of 20 °C, and the dimensions of the specimens were the same as those used in the LAS tests.

The effect of the strain amplitude, the rest time and the number of rest periods has been previously studied in [5]. The time sweep test with rest periods was implemented with a strain amplitude of 2.5 %, a rest time of 30 min and a sequence of 4 loading and 3 rest periods.

3.7. Healing indices

Based on previous work [5], three different healing indices were derived from other variables used to analyse the performance of the specimens in the test procedure, as follows: the complex shear modulus (*H*Im), the number of cycles to failure (*HIc*), and the VECD damage intensity (*HId*).

The index *H*Im after the rest period j is given by the complex shear modulus as:

$$HIm_j = \frac{|G^*|_{i+1_{initial}} - |G^*|_{i_{final}}}{|G^*|_{i_{final}}} \times 100 = \frac{\Delta|G^*|}{|G^*|_{i_{final}}} \times 100 \quad (5)$$

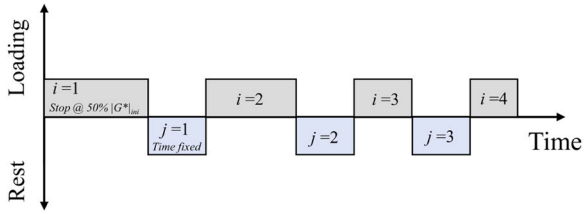

Fig. 1. Sequence of the time sweep test with rest periods.

where $|G^*|_{i+1_{initial}}$ is the initial complex shear modulus of loading period $i + 1$ (post rest j), and $|G^*|_{i_{final}}$ is the final complex shear modulus of loading period i (before rest j).

The index *HIc* after the rest period j is determined with the number of loading cycles as:

$$HIc_j = \frac{\Delta N_{i+1}}{N_1} \times 100 \quad (6)$$

where N_1 is the number of cycles of the first loading period, and ΔN_{i+1} is the number of cycles of loading period $i + 1$ (post rest j).

The index *HId* after the rest period j is determined with the damage as:

$$HId_j = \frac{S_{i+1}^F - S_i^F}{S_i^F} \times 100 \quad (7)$$

where S_i^F and S_{i+1}^F are the final S values of loading periods i and i-1, respectively. Fig. 2 illustrates the quantification of *HIm* , *HIc* and *HId* for the first rest period ($j = 1$).

4. Results

4.1. Geometric and chemical properties of fillers

Fig. 3 shows SEM images of limestone and steel slag filler particles obtained at different resolution levels. Despite the distinct origin of the fillers, a similar particle morphology is observed for both fillers. Most particles have an angular shape with a smooth to slightly rough texture. The granular shapes seen in the lower-resolution images appear to be agglomerates of particles formed during the preparation of the sample for SEM examination. Both fillers are very fine, with some particles smaller than 0.5 μm. Slightly larger particles were observed in the SEM images of the limestone filler. The similarity in the morphology and size of the particles in the two types of filler are related to the properties of the steel slag and the grinding process. On the contrary, Zhang *et al.* [24] observed very different surface morphologies by SEM for steel slag and limestone powder. The steel slag particles were irregularly shaped and had a rough texture with many pores, whereas the limestone particles were smoother and had fewer pores.

In addition, the geometric characteristics of the two tested fillers are consistent with the voids in compacted filler samples, as shown in Table 2, which are relatively similar. The voids in compacted filler, also referred to as Rigden voids, are influenced by the size and shape of the filler particles and serve as a good indicator of the filler's stiffening potential. The literature, e.g. in [47], reports very high Rigden voids values, sometimes exceeding 70 % for certain industrial products such as hydrated lime.

Fig. 4 shows the chemical composition analysis of the fillers obtained by EDS. The height (*y*-axis value) represents the intensity or photon count, which refers to the number of X-rays detected at each energy level. This intensity is directly proportional to the number of atoms of a particular element in the sample. The *x*-axis represents the energy of the X-ray photons in kiloelectron volts (keV). Each element emits X-rays at specific characteristic energies when its atoms are excited and then relax to lower energy states. *Ka* and *Kb* (which appear next to the chemical elements in the diagram) are designations for specific spectral lines that appear in X-ray spectroscopy, occurring due to the emission of X-rays when electrons from higher levels fall into the K-shell, the innermost shell of an atom. Similarly, *Li* and La are names for other spectral lines that appear in X-ray spectroscopy, produced by the emission of X-rays when electrons from higher levels fall into the L-shell.

The limestone filler is composed mainly of carbon (C), oxygen (O), and calcium (Ca), as expected. The presence of magnesium (Mg), aluminium (Al), silicon (Si) and traces of yttrium (Y) was also noted, confirming its mineralogical nature. In contrast, the chemical

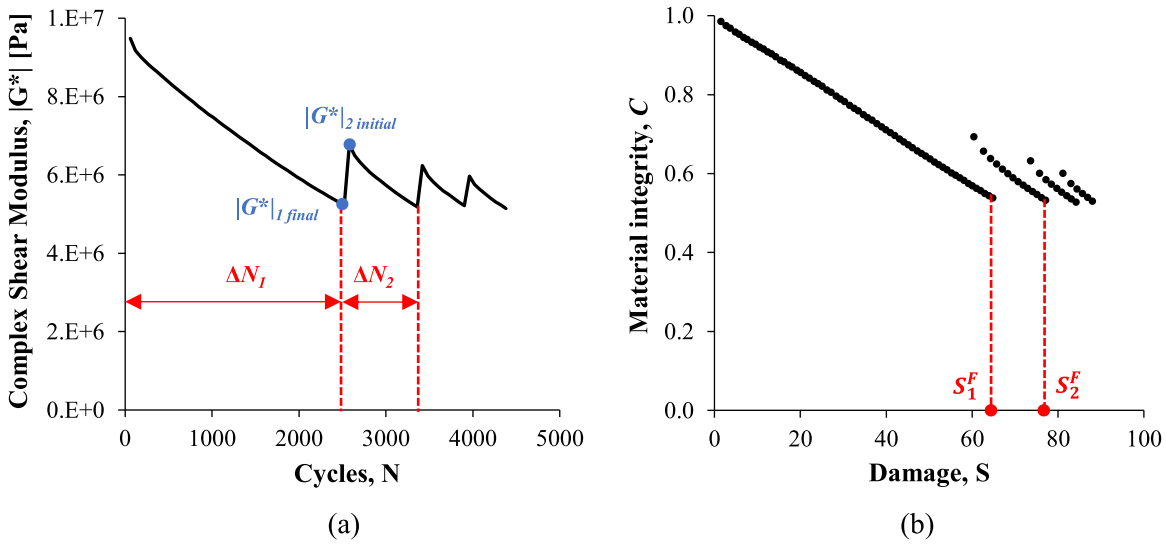

Fig. 2. Identification of variables for the calculation of healing indices: (a) HIm_1 and HIc_1; (b) HId_1.

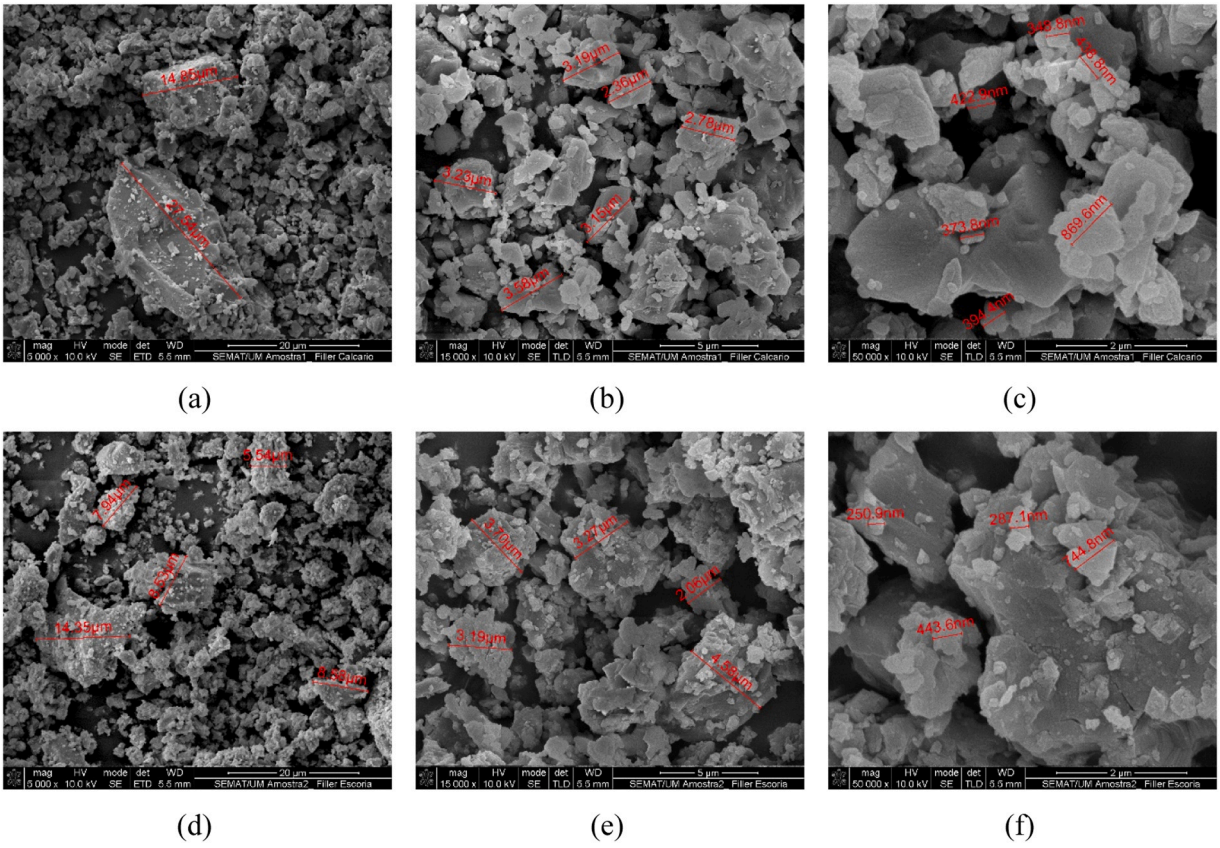

Fig. 3. SEM images of limestone filler ((a), (b) and (c)) and steel slag filler ((d), (e) and (f)) at different resolution levels (5000x, 15000x and 50000x).

composition of the steel slag is more diverse than that of limestone. The most abundant elements in steel slag are carbon (C), oxygen (O), iron (Fe), calcium (Ca), and silicon (Si). Magnesium (Mg), aluminium (Al), titanium (Ti), chromium (Cr), and manganese (Mn) are also observed.

The diversity in the chemical composition of steel slag can help improve bituminous materials' performance due to its effect on the adhesion between aggregate and bitumen. Similarly to limestone, steel slag is rich in Ca, and some calcium compounds, such as CaO and Ca $(OH)_2$, form insoluble salts by reacting with the organic acids in bitumen, improving water resistance [17]. In addition, other chemical compounds such as SiO_2 and Al_2O_3 can form strong intermolecular bonds with the molecular groups of bitumen through van der Waals forces, and even stronger than those of calcium compounds [24].

Both the chemical composition and the size, shape and surface characteristics of steel slag particles suggest that mastics with this filler can have strong filler-to-bitumen adhesion and water resistance.

4.2. *Consistency and rheological behaviour*

This section presents the results of the analysis of the physical

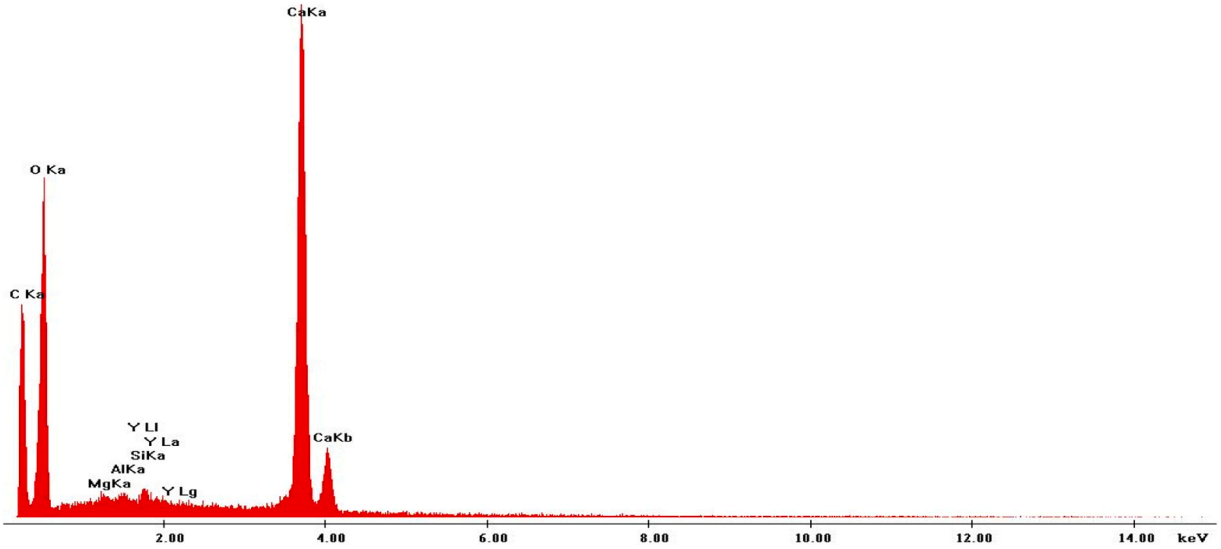

(a) Limestone Filler

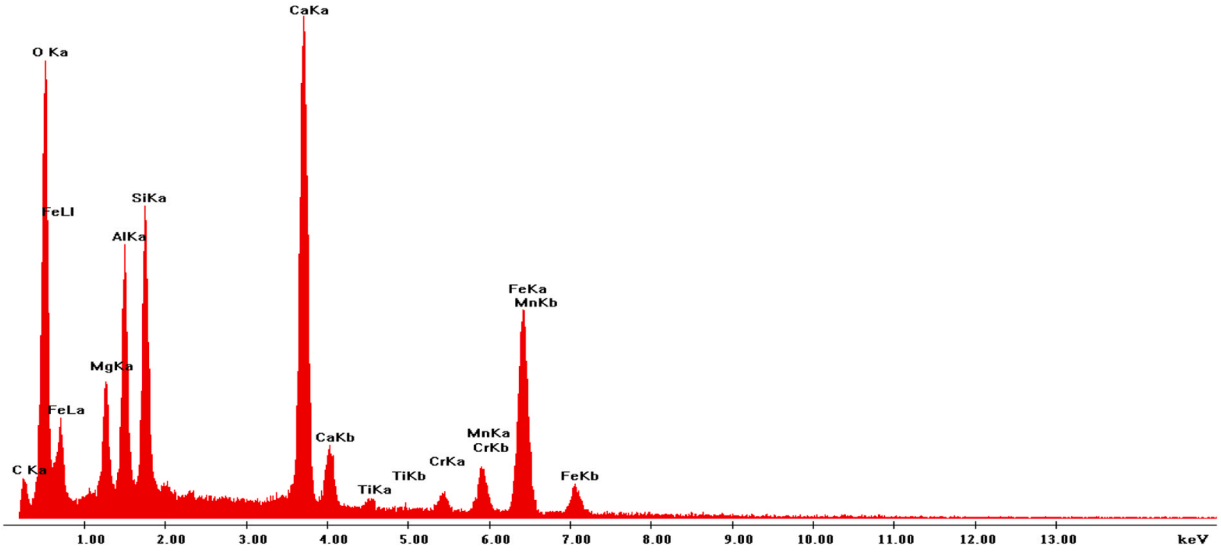

(b) Steel Slag Filler

Fig. 4. Composition analysis by energy-dispersive X-ray spectroscopy.

properties and rheological characterisation. Figs. 5(a) and 5(b) shows the effect of the filler type, the oxidative ageing and the bio-oil content on the consistency of the mastics, measured by the needle penetration at 25 ºC and softening point. For the consistency at intermediate temperatures, shown in Fig. 5(a), the needle penetration value increases with the bio-oil content, following approximately an exponential law, for the mastics with the bitumen aged to different degrees and containing the two fillers. A greater influence of the bio-oil is observed within the tested interval than for the other test variables (bitumen ageing and filler). Conversely, the needle penetration decreased significantly with increasing oxidative ageing in the bitumen, and this effect was greater at higher bio-oil contents. However, the effect of the filler was most significant for the unaged bitumen. On average, the needle penetration increased by 8 mm/10 for each 1 % of bio-oil added to the mastic, while it decreased by 7 mm/10 for each ageing treatment cycle. Mastics containing steel slag filler exhibited a needle penetration that was 2 mm/10 lower.

The needle penetration (*pen*) (mm/10) can therefore be expressed mathematically as follows:

$$pen = \left(a_1 \times e^{a_2 \times BO}\right) \times \left(a_3 + a_4 \times AGED\right) \quad (8)$$

where, e is the Euler number, BO is the rejuvenator content (%); $AGED$ is the degree of ageing (unaged = 0; RTFOT = 1 and PAV = 2); a_1, a_2, a_3 and a_4 are statistically determined coefficients. Fig. 5(a) shows a good adjustment of the model to the experimental data. Also, the fitted coefficients in Table 3 are similar for the two fillers, confirming the small effect of this variable.

The softening point indicates the temperature at which the bituminous material softens beyond a specific limit, and the test results show the opposite trend to the needle penetration for the variables studied. The temperature decreases with the bio-oil content, following an approximate linear law, and increases with ageing. The effect of the filler type was small. Contrary to the needle penetration, no greater effect of ageing was observed for higher bio-oil contents. On average, the softening point decreased by 2.5 ºC for each 1 % of bio-oil added to the

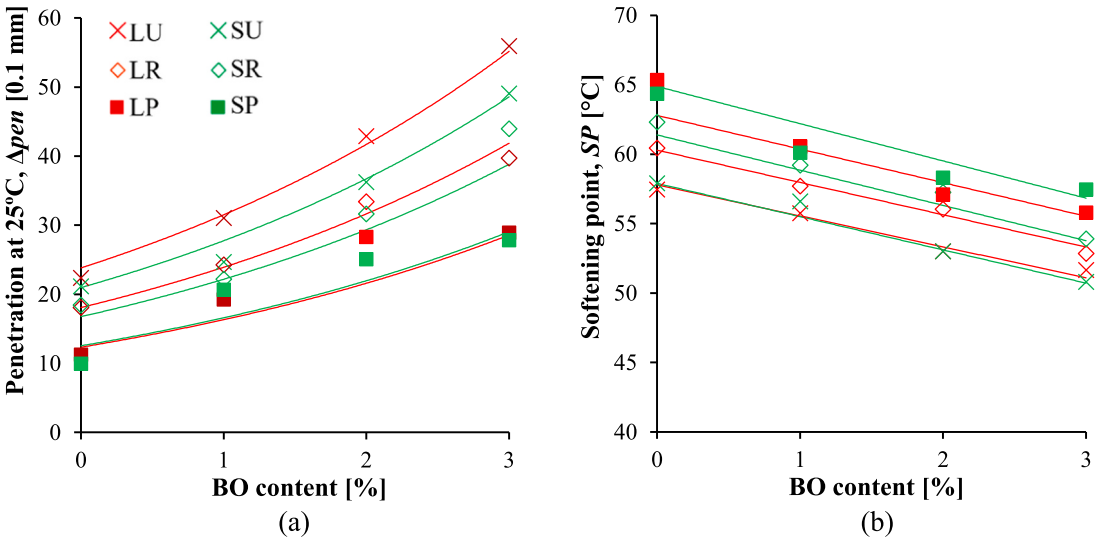

Fig. 5. Consistency test results and models (marker – test results; line – Eqs. (8) and (9)): (a) needle penetration; (b) softening point.

Table 3
Coefficients for Eq. (8).

Filler	a_1	a_2	a_3	a_4	R^2
Limestone	1.98	0.28	12.03	−2.90	0.99
Steel slag	1.81	0.28	11.59	−2.33	0.99

mastic, while it increased by 2.7 °C for each ageing treatment cycle. Mastics containing steel slag filler exhibited a softening point that was 0.6 °C higher.

Based on the results obtained, the softening point (SP) (°C) can be expressed as follows:

$$SP = (b_1 + b_2 \times BO) \times (b_3 + b_4 \times AGED) \quad (9)$$

where, b_1, b_2, b_3 and b_4 are statistically determined coefficients. The variables BO and AGED are defined as in Eq. (8). Table 4 shows the fitting coefficients determined for mastics with different fillers. Fig. 5(b) shows a good adjustment of the model to the experimental data.

To characterise the effect of filler type and bitumen, the linear viscoelastic (LVE) behaviour at 20 °C is summarised in Figs. 6 and 7. Fig. 6 illustrates the impact of the bio-oil on the complex shear modulus and phase angle for LU mastic (unaged bitumen and limestone filler). As expected, the bio-oil caused a decrease in the complex shear modulus and increased the viscous part of the viscoelastic behaviour. For the test conditions, the rheological behaviour of these materials was dominated by the viscous part (phase angle > 45 °), and the change in rheological properties is proportional to the bio-oil content.

Fig. 7 presents the complex shear modulus and phase angle measured at 10 Hz for all 24 mastics. For 3 % bio-oil incorporation, the $|G^*|$ value decreased by 64–75 %, and the δ value increased by 22–35 %. Thus, the bio-oil tested, derived from the biodiesel production process, showed a remarkable ability to reverse the ageing effects of the bitumen and the addition of 2 % was found to be sufficient to change the $|G^*|$ and δ values to those of the mastics with unaged bitumen. In addition, a significant variation in $|G^*|$ and δ values is observed due to the change in filler type and ageing treatment, which means a combination of effects

Table 4
Coefficients for Eq. (9).

Mix	b_1	b_2	b_3	b_4	R^2
Limestone	17.89	−0.69	3.23	0.14	0.99
Steel slag	18.38	−0.76	3.15	0.19	0.99

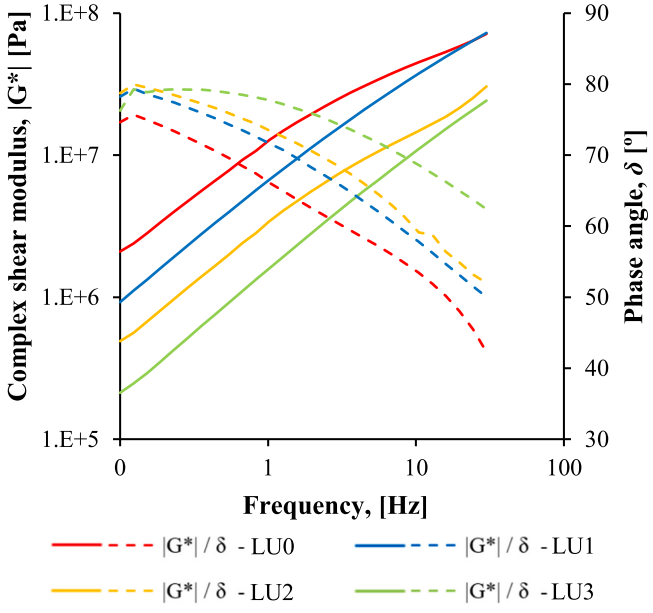

Fig. 6. Effect of frequency on LVE properties at 20 °C - *LU* samples.

of the studied variables. For example, from the unaged state to the long-term aged state of the bitumen, the $|G^*|$ value decreased by 27–152 % and the δ value increased by 4–23 %, and the mastics with steel slag were 5–40 % stiffer with a phase angle varying from −5–10 %. These results show that oscillatory dynamic measurements should be used to evaluate the effect of different constituents on the rheological behaviour of bituminous mastics. They also suggest that the bitumen volume immobilised by the filler particles due to physiochemical mechanisms was different depending on the oxidative ageing of the bitumen and the added bio-oil.

In a previous study [5], the effect of this bio-oil on bitumen was evaluated. It was found that for every 1 % addition of bio-oil, needle penetration increased by approximately 30 %, while the softening point decreased by 2 °C. Additionally, with 3 % bio-oil at 10 Hz, the $|G^*|$ value was reduced by 77 %, and the δ value increased by 18–30 %, depending on the ageing level of the bitumen. These results suggest that the bio heating oil has a consistent softening effect on the consistency and rheological properties of bitumen, regardless of the filler type used.

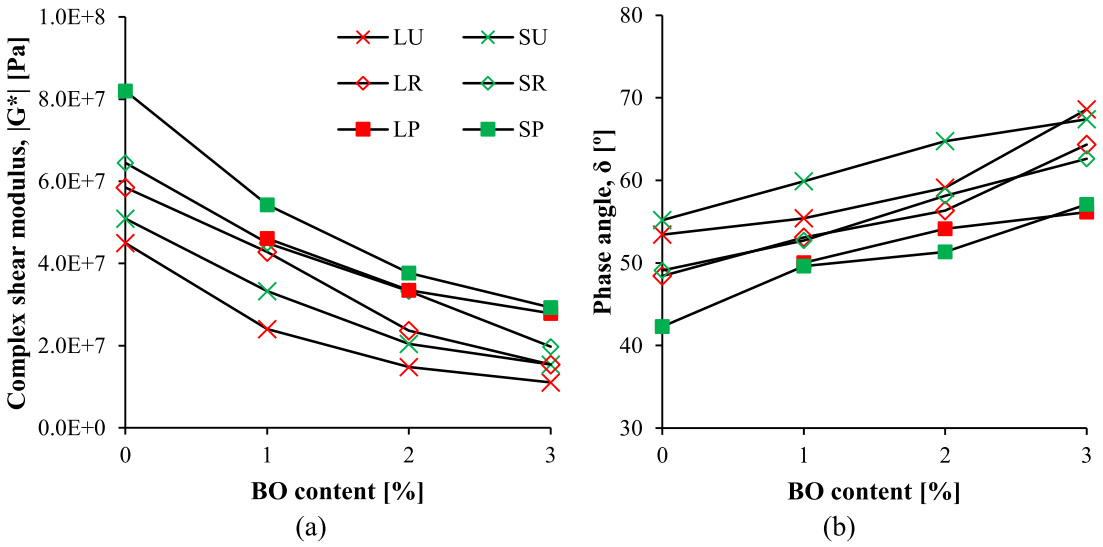

Fig. 7. Effect of BO content on LVE properties at 20 °C and 10 Hz: (a) $|G^*|$; (b) δ.

4.3. Fatigue resistance

This section presents the results of the fatigue resistance analysis of the mastics based on the LAS and TST-RP tests (see section 3.2.4). Fatigue resistance is critical for assessing the long-term performance and durability of bituminous materials under repeated loading conditions.

The LAS test is a cyclic test protocol that applies continuously increasing load amplitudes. Fig. 8(a) shows the evolution of the shear stress with the applied shear strain for LU specimens with increasing bio-oil content. The stress-strain trend followed the same bell-shaped curve for different samples. However, the maximum stress reached during the test was lower for samples with higher bio-oil content and subsequently decreased more slowly with strain. Hence, the point at which the maximum stress level is reached is often adopted to identify specimen failure in the LAS test [48–50].

Fig. 8(b) presents the strain amplitude applied at the maximum stress point (τ_{max}) for the different mastics. For the stiffest mastics, the test was not performed either because the shear stress reached the limit of the test equipment, or the sample broke very suddenly. The shear strain values varied between 4.8 % and 7.2 %, which are small values, and the range of variation is modest. The maximum shear strain increased with the bio-oil content, especially at 2 % and 3 %. Conversely, the yield point was reached earlier in the test for the mastics with the bitumen subjected to oxidative ageing. On average, the mastics with the limestone filler presented higher shear strain. These results show that, as expected, the ageing treatment made the mastics harder and less ductile, with a reduced ability to withstand large deformations. Thus, this effect can be reversed by the addition of bio-oil.

Fig. 9(a) shows the damage characteristic curves (*C*-*S*) of LU mastics, with different bio-oil content, obtained by applying the VECD analysis method to the LAS test results. The initial integrity (*C*) is 1.0 and decreases with the load cycles, corresponding to the increase of the damage (*S*) variable. It should be noted that the *S* value required to obtain an equivalent reduction in *C* increases proportionally with the bio-oil content, meaning that these mastics can sustain greater damage. Fig. 9 (b) shows the variation of the area under the *C*-*S* curve with the bio-oil content for the different mastics. The area increased with the bio-oil content and decreased with the ageing level. For example, for the mastic with limestone filler, the area increased by 18.7 % for each 1 % bio-oil content and decreased by 13.4 % and 30.3 % after the short- and long-term ageing treatments, respectively. Similarly, the *C*-*S* area of the mastics with steel slag was 11.9 % smaller. The incorporation of 2 %

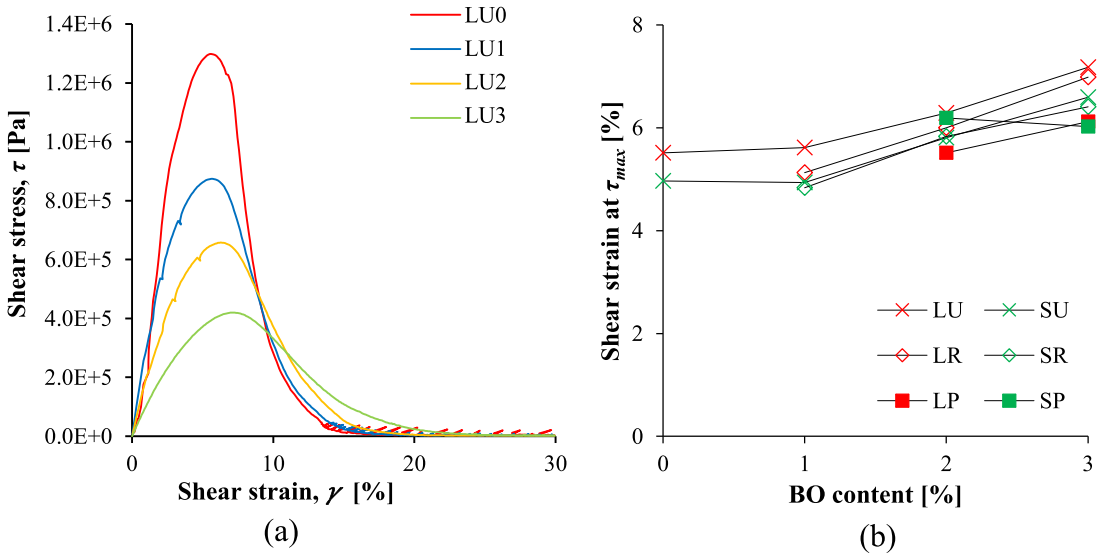

Fig. 8. LAS test results: (a) stress-strain curves – LU; (b) shear strain at τ_{max}.

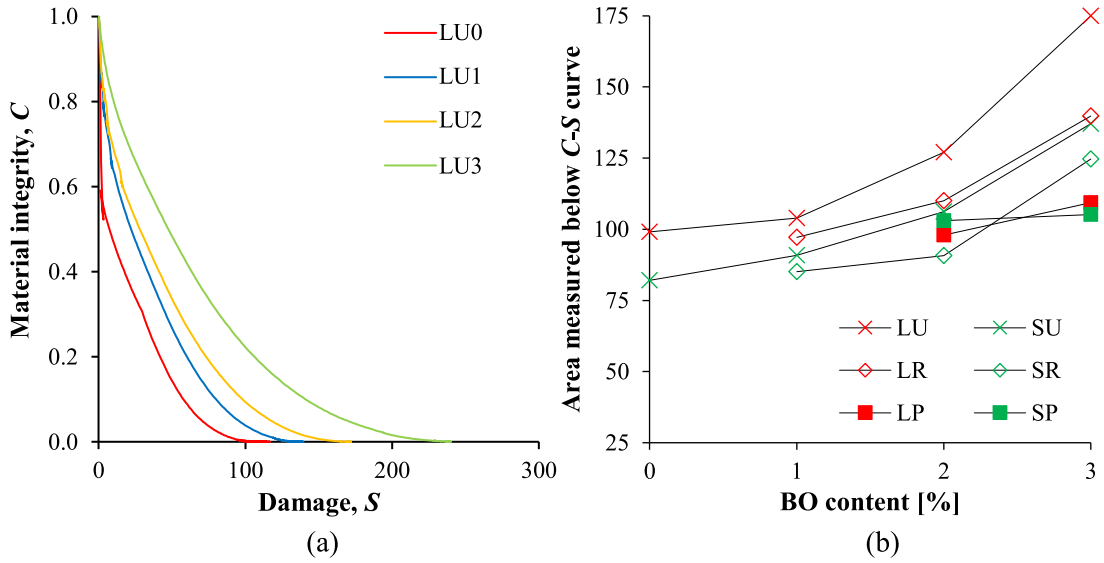

Fig. 9. Damage characteristic curves (*C-S*): (a) curves of LU samples; (b) area.

bio-oil in mastics with aged binders was sufficient to increase the area to that of mastics with unaged bitumen.

To compare the fatigue resistance evaluated with the LAS test, the number of cycles to failure at two different strain amplitudes (2.5 % and 5.0 %) is plotted in Fig. 10. Except for the mastic LR with 2 % and 3 % bio-oil, the fatigue resistance generally increased with the bio-oil content and decreased with bitumen ageing. For stiffer materials, the shear stress increases faster with the applied strain, which cannot relax the stresses due to continuous loading, and the specimen fails at small deformations due to the generally lower ductility. In the LAS test, the specimen fails due to the growth of radial microcracks from the outer edge to the centre, which reduces the effective section. Thus, the presence of solid particles, although very fine, and the amount of immobilised bitumen around them affect the crack growth and the overall fatigue resistance. The variation values are highly variable when comparing the mastics with different fillers. Still, the mastics with steel slag are expected to fail, on average, with less cycles (-5 %) than those with limestone filler.

Time sweep tests with rest periods were used to assess the healing ability of mastics. The test conditions were a temperature of 20 °C, a strain amplitude of 2.5 % and a loading frequency of 10 Hz. Fig. 11 shows the evolution of the complex shear modulus, normalised to its initial value, over four loading periods. The loading periods were interrupted for 30 minutes when the complex shear modulus had decreased to half the undamaged complex shear modulus value. In all cases, the number of cycles in each loading period decreased compared to the previous loading period, which can be attributed to the cumulative damage after the rest intervals. The bio-oil content in the samples obviously affected the fatigue resistance. Thus, the number of cycles the specimens withstood during the test, either considering only the first loading period or the entire test protocol, increased with the bio-oil content.

In contrast, the ageing effect had a less clear influence on the number of cycles to failure. The mastics with unaged binders withstood more extended loading periods for both mastics without bio-oil. The same trend was generally observed for the mastics with steel slag and bio-oil added. However, the fatigue resistance of the short-term aged material was higher for mastics with limestone filler and bio-oil. These results suggest that although bio-oil can reduce the stiffness and increase the fatigue resistance of mastics with aged binders, depending on the type of

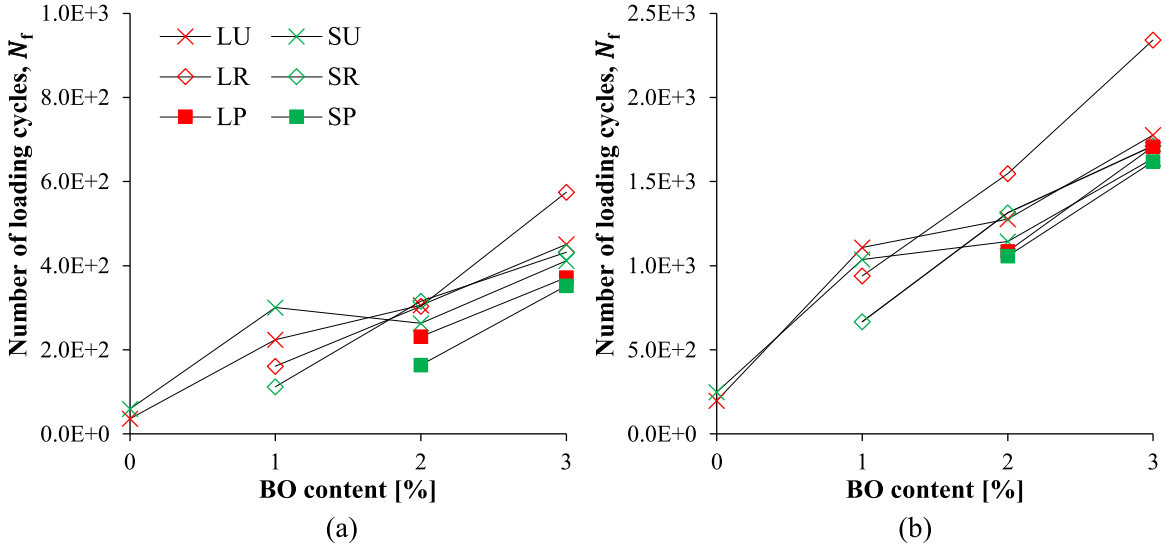

Fig. 10. Fatigue resistance estimated from LAS test at strain amplitude: (a) 2.5 %; (b) 5.0 %.

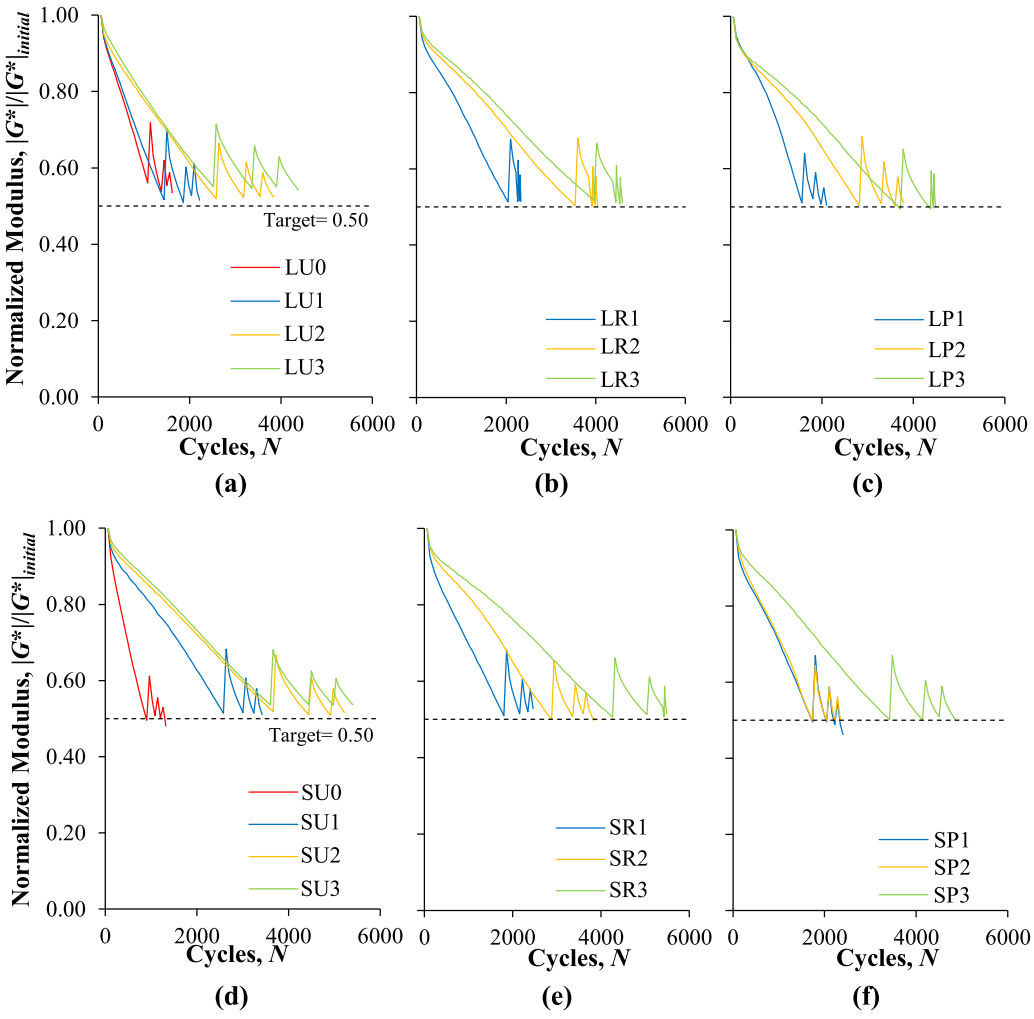

Fig. 11. Evolution of the normalised complex shear modulus with loading cycles: (a) LU; (b) LR; (c) LP; (d) SU; (e) SR; (f) SP.

filler, the fatigue resistance is not fully restored or further improved compared to materials with unaged binders.

On average, the total number of cycles in the four loading cycles increased by 89.7 % with each 1 % bio-oil addition and 9.0 % with the partial replacement of limestone filler by steel slag powder. It also decreased by 14.1 % with the increase in oxidative ageing induced by the PAV protocol (long-term).

In addition, Fig. 12 compares the number of cycles to failure measured in the TST-RP, considering only the first loading period ($i = 1$), and estimated using the fatigue laws obtained from LAS testing. In all cases, the LAS-based estimate of the number of cycles was lower (on average −55.8 %) than that measured in the TST-RP. In the literature, some researchers [51] have shown that similar fatigue resistance values can be obtained from TST-RP and LAS. As shown in [52], differences in TST-RP and LAS analysis methods partially explain the variance. In this work, the TST-RP loading was interrupted when the

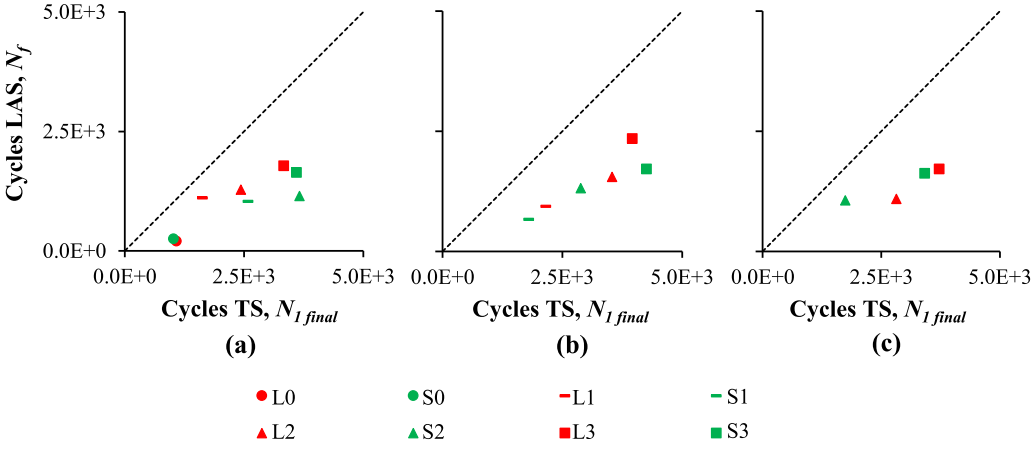

Fig. 12. Fatigue resistance ($\gamma = 2.5$ %), LAS *vs.* TST-RP (1st loading period): (a) LU and SU; (b) LR and SR; (c) LP and SP.

initial modulus had decreased by 50 % (C = 0.5), corresponding to the fatigue resistance. In contrast, in the analysis of the LAS results, the stress peak was allowed as an indication of the failure of the specimen, and up to this point, the C values were mostly higher than 0.5. The lower the C value for the fatigue resistance, the longer the estimated number of cycles to failure.

4.4. Healing contribution to mechanical properties

The results of the three healing indices (*HIm* , *HIc* and *HId*), determined from the time sweep tests with rest periods, are plotted in Figs. 13, 14 and 15. As described in Section 3.3, the *HIm* index measures the change in the complex shear modulus of the material before and after the rest period (Eq. (5)). The *HIc* index compares the duration (cycles) of the subsequent loading periods with the initial loading period (Eq. (6)), and the *HId* index evaluates the level of damage accumulated during the loading period after the rest period (Eq. (7)).

The number of loading periods is the most important factor in the recovery of the complex shear modulus during the rest period, as shown in Fig. 13. On average, the recovery of mastic with limestone filler is 29.7 %, 17.8 % and 12.4 % after the first, second and third rest periods, respectively. The results of the mastic with steel slag were also close to these values (absolute difference from 0.1 % to 1.3 %). Increasing oxidative ageing had only a slight effect, and mastic L was the opposite of that expected. Mastics L with aged bitumen had, on average, higher *HIm* values (+1.9 % after RTFOT and +1.5 % after PAV) than the corresponding mastics with unaged bitumen. For mastic S, these differences were −0.4 % after RTFOT and −0.1 % after PAV. The incorporation of bio-oil in mastics LU and SU increased the healing index by 7.3 % and 4.4 %, respectively. However, the effect of increasing further the bio-oil content (from 1 % to 3 %) on the healing index values is relatively small, except for LP (average 4.0 %) and SP (average 1.8 %).

Differently from the *HIm* index, healing during the rest period had a lesser effect on the loading period duration (number of loading cycles) than on the stiffness modulus, *i.e.*, the *HIc* values shown in Fig. 14 are significantly smaller than the *HIm* values shown in Fig. 13. The duration of the loading periods after resting was, on average, 13.4 % (16.8 %), 5.4 % (8.8 %) and 3.8 % (5.0 %) of the initial duration (1st) for mastic L (mastic S) for the 2nd, 3rd and 4th periods, respectively. In addition, the healing effect decreased further in the 2nd and 3rd resting periods. As expected, oxidative ageing had a negative impact on the healing ability of the mastics. On average, the short-term aged mastics had the lowest *HIc* values (-8.3 % (L) and −2.9 % (S) relative to the unaged mastics), even lower than those of the mastics with the long-term aged bitumen. Mastic with steel slag had higher *HIc* values (10.4 % ± 5.7 %) than mastic with limestone filler (7.9 % ± 6.1 %). For both mastics with unaged bitumen (LU and SU), the addition of only 1 % of bio-oil did not improve the healing index values when compared to mastic without bio-oil, but the *HIc* values increased for 2 % and 3 % bio-oil contents (+4.7 % (L) and + 2.8 % (S) of 3 % relative to 1 %).

In general, it is observed in Fig. 15 that the *HId* values are closer to the *HIc* values than to the *HIm* values. Similarly to the observations for

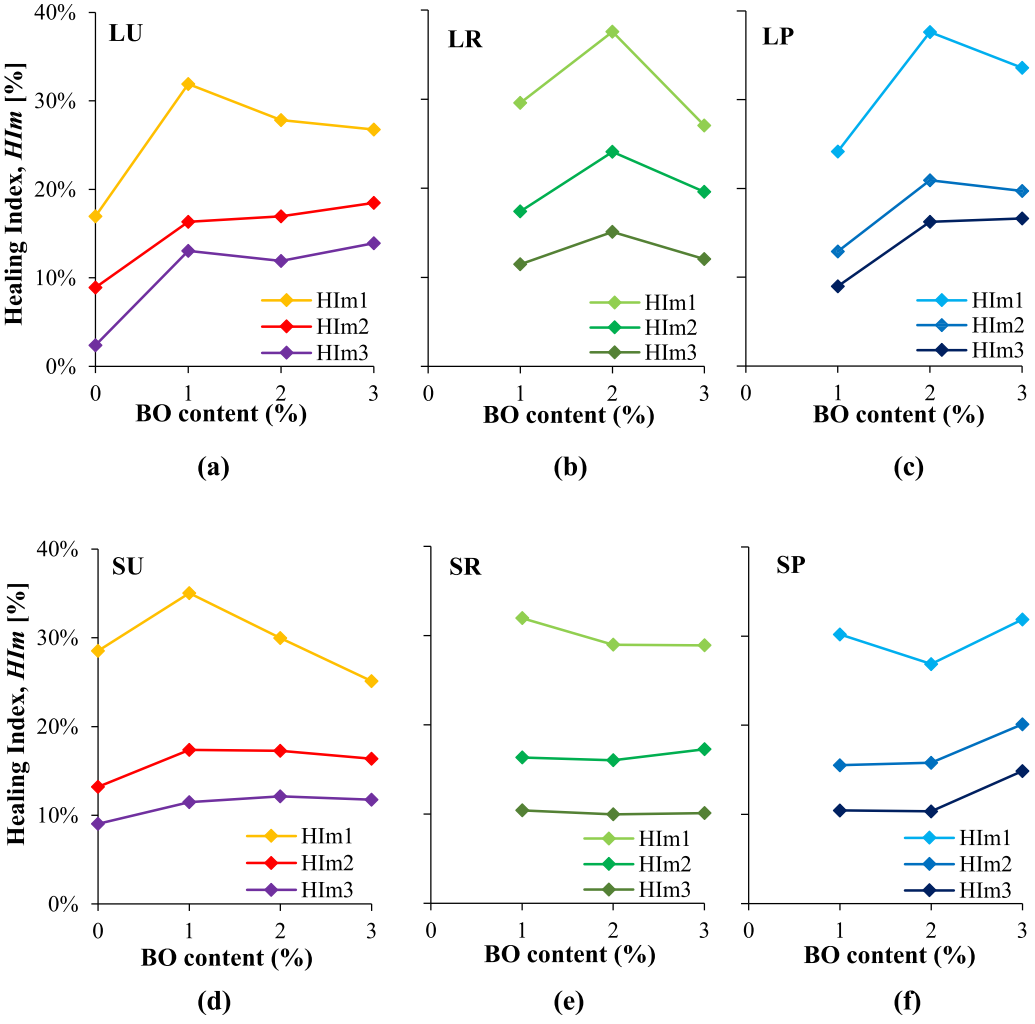

Fig. 13. Healing index *HIm* : (a) LU; (b) LR; (c) LP (d) SU (e) SR (f) SP.

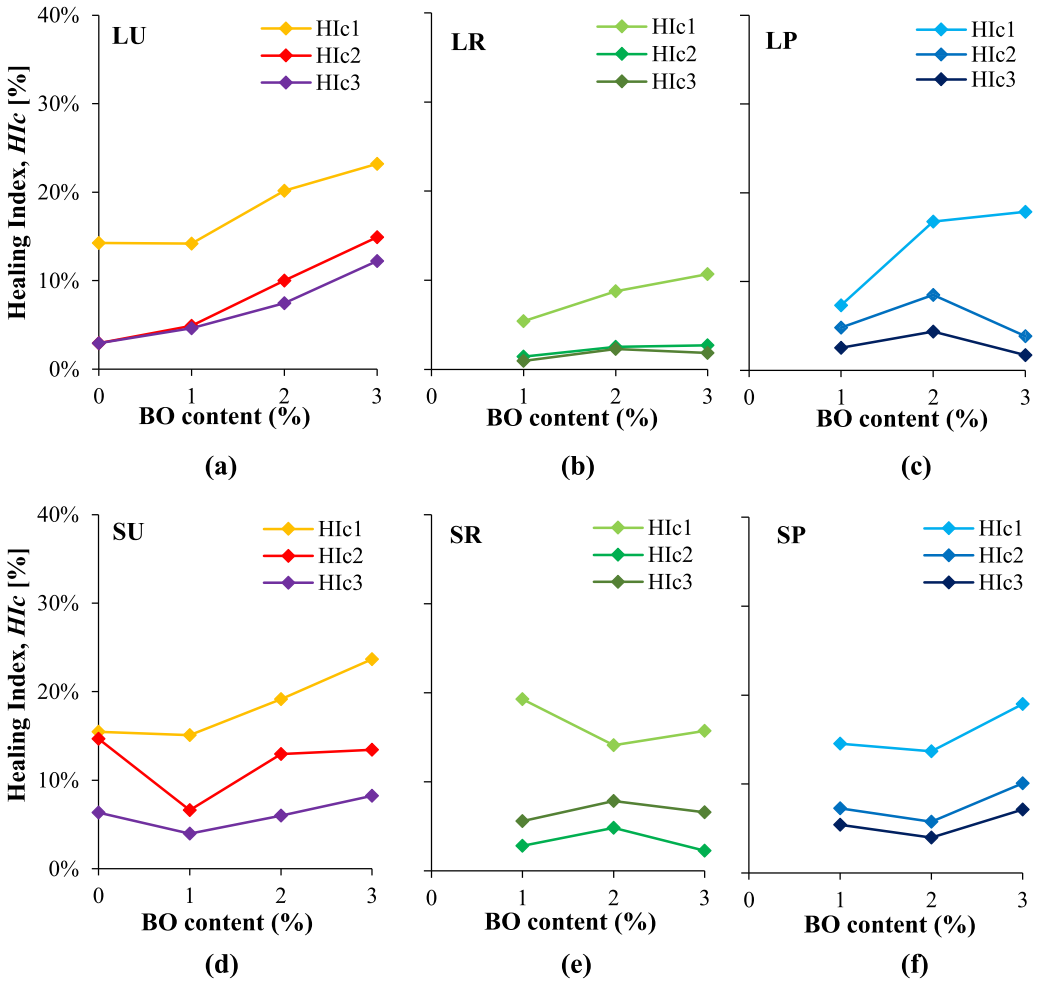

Fig. 14. Healing index *HIc*: (a) LU; (b) LR; (c) LP (d) SU (e) SR (f) SP.

the other indices, the *HId* values decreased significantly with the accumulation of loading periods, from an average of 15.3 % and 14.3 % after the 1st rest period, to 3.5 % and 2.8 % after the 3rd rest period for mastics L and S, respectively. The effects of the filler type, the ageing level of bitumen and the bio-oil content were significantly less important for the *HId* values. Thus, the values for mastic L are only slightly higher (average difference +0.5 %) than those for mastic S. The mastics with long-term aged mastic had the lowest healing values (average difference to unaged mastic −1.2 % (L) and −2.0 % (S)), and the increase from 1 % to 3 % bio-oil resulted in a difference of + 5.4 % (L) and + 4.8 % (S).

To further support the analysis of the effect of the different variables on the healing indices, a model was fitted to the data of mastics with different fillers as follows:

$$HI = (c_1 + c_2 \times BO) \times \left(c_3 \times e^{c_4 \times (LOAD-1)}\right) \times (c_5 + c_6 \times AGED) \quad (10)$$

where, *HI* is the healing index (%) (HIm, Hic and HId); *BO* is the increase in rejuvenator content (%); *LOAD* is the number of loading periods (2, 3 and 4); *AGED* is related to the aged level (unaged = 0; RTFOT = 1 and PAV = 2); c_1, c_2, c_3, c_4, c_5 and c_6 are statistically determined coefficients (fitting coefficients listed in Table 5). The linear and exponential models expressing the effect of each variable were defined based on the analysis of Figs. 13, 14 and 15, which had a very good fit to data (R^2 values from 0.83 to 0.97).

The model was used to perform a sensitivity analysis, as shown in Table 6. This involved applying a variation to the input parameters, to assess their effect on the mastic healing results. The coefficient of variation (CV_{HI}) was determined as (HI_2 – HI_{ref}) / HI_{ref}, where HI_{ref} is the healing index value for the reference conditions, and HI_2 is the healing index value for the varying conditions. The CV_{HI} values show the strong effect of the number of loading periods on all indices (see cases *ii* and *v*). Except for the *HIc* mastic with limestone filler, the bio-oil content has a significant effect on the healing indices (see cases *i* and *iv*). Based on cases iii and vi, the *HIm* values increase with the degree of ageing, although less than that of the other factors, and the opposite trend occurs with the other indices.

From the above comments, it is clear that the three healing indices do not provide a uniform evaluation of healing in bituminous mastics, and that the number of loading periods plays a significantly more important role than the variations in material composition. According to the Rilem Technical Committee TC 278-CHA (Crack-Healing of Asphalt Pavement Materials) [53], the loss of stiffness and strength properties due to cyclic loading occurs not only from damage but also from mechanisms related to the time- and temperature-dependant nature of bituminous materials (*e.g.* thixotropy, relaxation and redistribution of stresses). Consequently, the total observed change in mechanical properties after a period of rest, referred as restoration, is the sum of changes related to the removal of cyclic loading and the closure and repair of micro-cracks. Hence, it is not simple to separate their individual contributions.

In this study, the three healing indices do not explicitly distinguish between these two mechanisms of restoration, though it is likely that their relative influence differs across the indices. The *HIm* index showed significantly higher values than the other two indices (*HIc* and *HId*), indicating that it is more affected by recovery mechanisms associated with the removal of cyclic loading than by actual damage repair. While heating is less relevant in DSR testing due to the small specimen

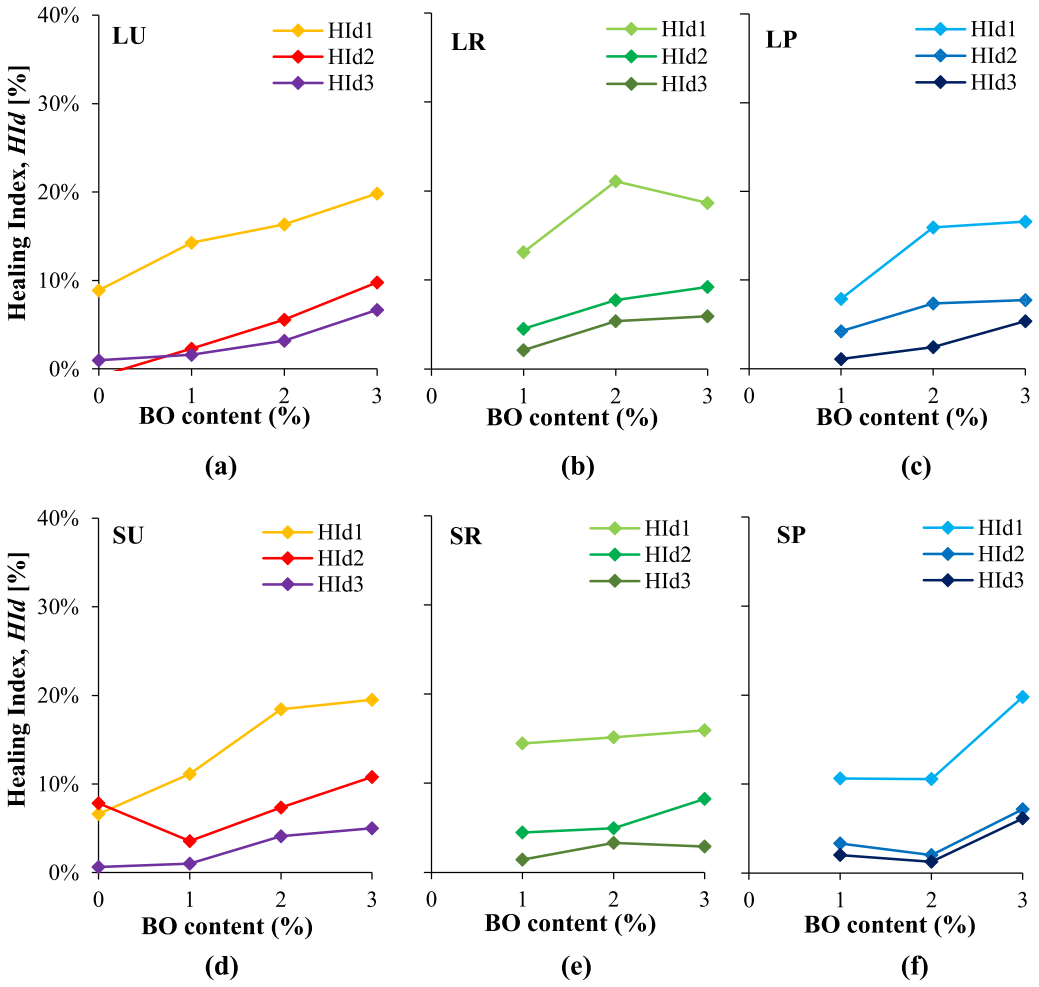

Fig. 15. Healing index *HId*: (a) LU; (b) LR; (c) LP (d) SU (e) SR (f) SP.

Table 5
Coefficients for Eq. (10).

HI	Filler	c_1	c_2	c_3	c_4	c_5	c_6	R^2
HIm	L	0767	0.259	−0.051	−0.469	−5.918	−0.466	0.98
	S	0.225	1.361	−0.016	−0.463	−5.842	−0.693	0.80
HIc	L	0.183	0.037	−0.075	−0.852	−11.712	1.066	0.83
	S	0.307	0.331	−0.057	−0.536	−5.402	0.689	0.97
HId	L	0.055	0.213	−0.061	−0.832	−12.004	0.493	0.95
	S	0.126	0.172	−0.094	−0.985	−10.644	0.934	0.96

Table 6
Sensitivity analysis of healing test.

	BO	*LOAD*	*AGED*	L	S	L	S	L	S
	Reference (ref) condition			*HIm* (%)		*HIc* (%)		*HId* (%)	
	1	3	1	13.1	6.6	3.2	5.9	3.6	3.8
Case	Input parameters			Coefficient of variation CV_{HI}					
i	2	3	1	25.2 %	85.8 %	16.8 %	51.9 %	79.5 %	57.7 %
ii	1	4	1	−37.4 %	−37.1 %	−57.3 %	−41.5 %	−56.5 %	−62.7 %
iii	1	3	2	7.3 %	10.6 %	−10.0 %	−14.6 %	−4.3 %	−9.6 %
iv	0	3	1	−25.2 %	−85.8 %	−16.8 %	−51.9 %	−79.5 %	−57.7 %
v	1	2	1	59.8 %	58.9 %	134.4 %	70.9 %	129.8 %	167.8 %
vi	1	3	0	−7.3 %	−10.6 %	10.0 %	14.6 %	4.3 %	9.6 %

size, unlike bituminous mixture testing [54], viscoelastic mechanisms remain relevant. Under an imposed deformation that does not cause immediate failure, the bitumen undergoes molecular reorganization that reduces its stiffness [55]. Nonlinear behaviour accounts for the immediate stiffness loss during loading, while thixotropy explains the progressive loss under continued loading. This thixotropic effect diminishes during rest, contributing to the observed stiffness recovery. However, the rate of microstructural rebuilding (recovery) can vary

depending on temperature and the material's properties [56].

Thus, the improved recovery of stiffness modulus, as quantified by *HIm* in certain aged materials (e.g., mastics with limestone filler), suggests that the observed effect is largely due to cyclic loading removal rather than micro-crack healing. This is because mechanisms such as flow and crack closure are less likely in materials that behave more elastically and are more brittle, such as aged bituminous materials [57]. Furthermore, oxidative ageing promotes stronger intermolecular interactions, leading to the formation of more colloidal gel structures. These structures enhance thixotropic behaviour by requiring more time to break down under shear and more time to recover afterward [58,59].

Unlike the *HIm* index, which reflects only stiffness variation after the rest period, the *HIc* and *HId* indices measure the length of the loading period following rest. As a result, they are more sensitive to viscoelastic flow, diffusion, and recrystallization mechanisms that contribute to micro-crack healing. These mechanisms can help prolong the number of cycles the material withstands before reaching the failure criterion. Consequently, both *HIc* and *HId* indices showed a reduction in healing with oxidative ageing, especially for the intermediate level (RTFOT), and an improvement with increasing bio-oil content.

Oxidative ageing induces significant alterations in the chemical composition of bitumen, particularly in the distribution of functional groups that govern its viscoelastic behavior, ductility, elastic recovery, and flow characteristics. These properties are critical for ensuring optimal performance across varying environmental and loading conditions [42,60,61]. To mitigate these effects, an effective rejuvenator must restore the aged bitumen by re-establishing the original chemical balance and improving its rheological and performance-related characteristics.

Sun et al. [62]and Gaudenzi et al. [63] observed that both aging and the addition of rejuvenators positively influenced the healing index at intermediate temperatures (approximately 20 °C). However, Sun et al. further reported that at elevated temperatures (25–30 °C), aging had an adverse impact on healing performance. Based on these findings, they proposed the concept of a healing–temperature curve specific to each bitumen, suggesting that variations in healing behavior could be attributed to elastic recovery at lower to intermediate temperatures and flow capacity at higher temperatures. Furthermore, the authors indicated that aging tends to shift this healing–temperature curve toward lower temperatures, while the application of rejuvenators causes a shift in the opposite direction.

In addition, the results showed a modest contribution of healing in terms of fatigue resistance, possibly because the damage induced during the first loading cycle was too significant for the physicochemical mechanisms (flow, wetting, diffusion and randomisation) [57] to be effective under the test conditions (30 min at 20 ºC).

5. Conclusions

This paper presents a study investigating the healing behaviour of bituminous mastics modified with bio-oil derived from biodiesel production, focusing on the effect of the bio-oil content, the degree of ageing of the bitumen and the replacement of the limestone filler by steel slag filler. The bituminous mastics were characterised relative to the consistency, the linear viscoelastic behaviour and the fatigue performance using two different test methods: linear amplitude sweep test and time sweep test with rest periods. Three healing indices were used to evaluate the healing ability during the rest periods of the different compositions of the mastics, as follows: *HIm* (related to the recovery of the loss of stiffness modulus); *HIc* (related to the number of cycles in the post-rest loading periods); and *HId* (related to the increase in damage intensity in the post-rest loading periods). The main findings can be summarized as below:

- Results from the consistency and viscoelastic characterisation showed that all three variables had significant influence, ranked in the following order of importance: bio-oil content, oxidative ageing, and filler type. Incorporating 2 % bio-oil effectively reversed the effects of long-term ageing, restoring properties such as needle penetration and phase angle, while reducing stiffness and softening point increases. The combination of filler type and bitumen ageing significantly affected linear viscoelastic properties.
- In terms of fatigue resistance without considering healing, performance improved with increasing bio-oil content across both test methods. However, the influence of oxidative ageing and filler type varied depending on the mastic composition and test type. The LAS test estimated lower fatigue resistance compared to the first loading period of the TST-RP, indicating differences in test sensitivity.
- The rest periods prolonged the fatigue life of mastics (TST-RP). On average, the total number of cycles in the four loading cycles increased by 89.7 % with each 1 % bio-oil addition and 9.0 % with the partial replacement of limestone filler by steel slag powder. On the contrary, it decreased by 14.1 % with the increase in oxidative ageing induced by the PAV protocol (long-term).
- The healing analysis revealed that a 30-minute rest period at 20°C was insufficient to fully restore the undamaged state, and healing capacity diminished with each loading cycle. Among the indices, *HIm* showed the most sensitivity to rest period effects and was the only index to reflect a positive response to increased ageing. While *HIc* and *HId* values were similar in magnitude, their response to mastic composition differed. Bio-oil improved healing capacity in general, though the degree of improvement varied with mastic formulation and the specific healing index.
- The influence of filler type on healing capacity was relatively minor, but steel slag powder was shown to be a viable alternative to limestone filler. Although the physical characteristics of both fillers were similar, differences in their chemical properties led to varying interactions with aged bitumen, thereby influencing stiffness and cyclic loading resistance. Consequently, filler effects should be assessed case-by-case depending on binder and mixture composition.
- Based on the findings, further investigation into the healing behaviour of mastics incorporating steel slag and bio-oils under higher temperature conditions is recommended. This would allow for the assessment of thermal conductivity benefits in field-relevant scenarios.

CRediT authorship contribution statement

Marina Cabette: Writing – original draft, Investigation, Formal analysis. **Rui Micaelo:** Writing – review & editing, Supervision, Methodology, Investigation, Conceptualization. **Jorge Pais:** Writing – review & editing, Validation, Supervision, Resources, Investigation, Conceptualization.

Declaration of Competing Interest

The authors declare that they have no known competing financial interests or personal relationships that could have appeared to influence the work reported in this paper.

Acknowledgements

The authors gratefully acknowledge the Foundation for Science and Technology (FCT) for the financial support given to the first author (PhD grant reference SFRH/BD/144683/2019) and R&D units: Civil Engineering Research and Innovation for Sustainability (CERIS) (project UIDB/04625/2025); Sustainability and Innovation in Structural Engineering (ISISE) (project UIDB/04029/2025).

Data availability

Data will be made available on request.

References

[1] Á. García, Self-healing of open cracks in asphalt mastic, Fuel 93 (2012) 264–272, https://doi.org/10.1016/j.fuel.2011.09.009.

[2] G. Mazzoni, A. Stimilli, F. Cardone, F. Canestrari, Fatigue, self-healing and thixotropy of bituminous mastics including aged modified bitumens and different filler contents, Constr. Build. Mater. 131 (2017) 496–502, https://doi.org/10.1016/j.conbuildmat.2016.11.093.

[3] S. Zhang, J. Yue, J. Wu, R. Li, Influence of rock asphalt on self-healing behavior of asphalt mastics, Constr. Build. Mater. 310 (2021) 124851, https://doi.org/10.1016/j.conbuildmat.2021.124851.

[4] C. Santos, M. Cabette, J. Pais, V. Carvalho, P. Pereira, Assessing Self-healing Asphalt by the Heating of Asphalt Mixtures, in: C. Raab (Ed.), Proceedings of the 9th International Conference on Maintenance and Rehabilitation of Pavements—Mairepav9, Springer International Publishing, Cham, 2020, pp. 253–261, https://doi.org/10.1007/978-3-030-48679-2_25.

[5] M. Cabette, R. Micaelo, J. Pais, The use of bio-oil from biodiesel production for enhancing the bitumen healing, Constr. Build. Mater. 409 (2023) 134033, https://doi.org/10.1016/j.conbuildmat.2023.134033.

[6] Jose Norambuena-Contreras, Erkut Yalcin, Robin Hudson-Griffiths, Alvaro García, Mechanical and self-healing properties of stone mastic asphalt containing encapsulated rejuvenators, J. Mater. Civ. Eng. 31 (2019) 04019052, https://doi.org/10.1061/(ASCE)MT.1943-5533.0002687.

[7] Ö.E. Yamaç, M. Yilmaz, E. Yalçın, B.V. Kök, J. Norambuena-Contreras, A. Garcia, Self-healing of asphalt mastic using capsules containing waste oils, Constr. Build. Mater. 270 (2021) 121417, https://doi.org/10.1016/j.conbuildmat.2020.121417.

[8] Q. Liu, S. Wu, E. Schlangen, Induction heating of asphalt mastic for crack control, Constr. Build. Mater. 41 (2013) 345–351, https://doi.org/10.1016/j.conbuildmat.2012.11.075.

[9] C. Li, S. Wu, Z. Chen, G. Tao, Y. Xiao, Enhanced heat release and self-healing properties of steel slag filler based asphalt materials under microwave irradiation, Constr. Build. Mater. 193 (2018) 32–41, https://doi.org/10.1016/j.conbuildmat.2018.10.193.

[10] M. Cabette, J. Pais, R. Micaelo, Extrinsic healing of asphalt mixtures: a review, Road. Mater. Pavement Des. 25 (2024) 1145–1173, https://doi.org/10.1080/14680629.2023.2266506.

[11] M. Abedraba-Abdalla, A. Garcia-Hernández, F. Haughey, N. Thom, L. Li, One-year results of the first road surface with the addition of sunflower oil porous capsules, Constr. Build. Mater. 445 (2024) 137939, https://doi.org/10.1016/j.conbuildmat.2024.137939.

[12] P. Apostolidis, X. Liu, A. Scarpas, C. Kasbergen, M.F.C. van de Ven, Advanced evaluation of asphalt mortar for induction healing purposes, Constr. Build. Mater. 126 (2016) 9–25, https://doi.org/10.1016/j.conbuildmat.2016.09.011.

[13] C. Clopotel, H. Bahia, The effect of bitumen polar groups adsorption on mastics properties at low temperatures, Road. Mater. Pavement Des. 14 (2013) 38–51, https://doi.org/10.1080/14680629.2013.774745.

[14] Y. He, K. Xiong, J. Zhang, F. Guo, Y. Li, Q. Hu, A state-of-the-art review and prospectives on the self-healing repair technology for asphalt materials, Constr. Build. Mater. 421 (2024) 135660, https://doi.org/10.1016/j.conbuildmat.2024.135660.

[15] W. Buttlar, D. Bozkurt, G. Al-Khateeb, A. Waldhoff, Understanding asphalt mastic behavior through micromechanics, Transp. Res. Rec.: J. Transp. Res. Board 1681 (1999) 157–169, https://doi.org/10.3141/1681-19.

[16] P. Ekholm, E. Blomberg, P. Claesson, I.H. Auflem, J. Sjöblom, A. Kornfeldt, A Quartz crystal microbalance study of the adsorption of asphaltenes and resins onto a hydrophilic surface, J. Colloid Interface Sci. 247 (2002) 342–350, https://doi.org/10.1006/jcis.2002.8122.

[17] C.W. Curtis, K. Ensley, J. Epps, Fundamental properties of asphalt-aggregate interactions including adhesion and absorption, National Academy of Science, USA, 1993.

[18] P. Kumar, S. Shukla, Utilization of steel slag waste as construction material: A review, Mater. Today.: Proc. 78 (2023) 145–152, https://doi.org/10.1016/j.matpr.2023.01.015.

[19] A. Paixão, E. Fortunato, Abrasion evolution of steel furnace slag aggregate for railway ballast: 3D morphology analysis of scanned particles by close-range photogrammetry, Constr. Build. Mater. 267 (2021) 121225, https://doi.org/10.1016/j.conbuildmat.2020.121225.

[20] S. Gopinath, A. Mehra, Carbon dioxide sequestration using steel slag—modeling and experimental investigation, in: F. Pacheco-Torgal, C. Shi, A.P. Sanchez (Eds.), Carbon Dioxide Sequestration in Cementitious Construction Materials, 4, Woodhead Publishing, 2018, pp. 65–80, https://doi.org/10.1016/B978-0-08-102444-7.00004-6.

[21] M. Pasetto, A. Baliello, G. Giacomello, E. Pasquini, The use of steel slags in asphalt pavements: a state-of-the-art review, Sustainability 15 (2023) 8817, https://doi.org/10.3390/su15118817.

[22] Y. Meng, T. Yan, Y. Muhammad, J. Li, P. Qin, L. Ling, H. Rong, X. Yang, Study on the performance and sustainability of modified waste crumb rubber and steel slag powder/SBS composite modified asphalt mastic, J. Clean. Prod. 338 (2022) 130563, https://doi.org/10.1016/j.jclepro.2022.130563.

[23] G. Tao, Y. Xiao, L. Yang, P. Cui, D. Kong, Y. Xue, Characteristics of steel slag filler and its influence on rheological properties of asphalt mortar, Constr. Build. Mater. 201 (2019) 439–446, https://doi.org/10.1016/j.conbuildmat.2018.12.174.

[24] Q. Zhang, J. Luo, Z. Yang, J. Wang, Y. Zhao, Y. Zhang, Creep and fatigue properties of asphalt mastic with steel slag powder filler, Case Stud. Constr. Mater. 18 (2023) e01743, https://doi.org/10.1016/j.cscm.2022.e01743.

[25] Q. Dai, Z. Wang, M.R. Mohd Hasan, Investigation of induction healing effects on electrically conductive asphalt mastic and asphalt concrete beams through fracture-healing tests, Constr. Build. Mater. 49 (2013) 729–737, https://doi.org/10.1016/j.conbuildmat.2013.08.089.

[26] D. Grossegger, B. Gomez-Meijide, S. Vansteenkiste, A. Garcia, Influence of rheological and physical bitumen properties on heat-induced self-healing of asphalt mastic beams, Constr. Build. Mater. 182 (2018) 298–308, https://doi.org/10.1016/j.conbuildmat.2018.06.148.

[27] Y. Zhang, C. Si, T. Fan, Y. Zhu, S. Li, S. Ren, P. Lin, Research on the optimal dosage of Bio-Oil/Lignin composite modified asphalt based on rheological and Anti-Aging properties, Constr. Build. Mater. 389 (2023) 131796, https://doi.org/10.1016/j.conbuildmat.2023.131796.

[28] Z. Zhang, Y. Fang, J. Yang, X. Li, A comprehensive review of bio-oil, bio-binder and bio-asphalt materials: their source, composition, preparation and performance, J. Traffic Transp. Eng. (Engl. Ed. 9 (2022) 151–166, https://doi.org/10.1016/j.jtte.2022.01.003.

[29] M. Cabette, J. Pais, R. Micaelo, Effect of bio heating oil from biodiesel production on rheological behaviour of bitumen. in: Eleventh International Conference on the Bearing Capacity of Roads, Railways and Airfields, Volume 3, Inge Hoff, Helge Mork, Rabbira Garba Saba, CRC Press, 2022, p. 10, https://doi.org/10.1201/9781003222910-44.

[30] R. Zhang, H. Wang, X. Jiang, Z. You, X. Yang, M. Ye, Thermal storage stability of bio-oil modified asphalt, J. Mater. Civ. Eng. 30 (2018) 04018054, https://doi.org/10.1061/(ASCE)MT.1943-5533.0002237.

[31] R. Zhang, Z. You, H. Wang, M. Ye, Y.K. Yap, C. Si, The impact of bio-oil as rejuvenator for aged asphalt binder, Constr. Build. Mater. 196 (2019) 134–143, https://doi.org/10.1016/j.conbuildmat.2018.10.168.

[32] Y. Lei, H. Wang, X. Chen, X. Yang, Z. You, S. Dong, J. Gao, Shear property, high-temperature rheological performance and low-temperature flexibility of asphalt mastics modified with bio-oil, Constr. Build. Mater. 174 (2018) 30–37, https://doi.org/10.1016/j.conbuildmat.2018.04.094.

[33] CEN, EN 12607-1: Bitumen and bituminous binders - Determination of the resistance to hardening under the influence of heat and air - Part 1: RTFOT method, European Committee for Standardization, Brussels, 2014.

[34] CEN, EN 14769: Bitumen and bituminous binders - Accelerated long-term ageing conditioning by a Pressure Ageing Vessel (PAV), European Committee for Standardization, Brussels, 2012.

[35] CEN, EN 1426:2015. Bitumen and bituminous binders – Determination of needle penetration, European Committee for Standardization, Brussels, Belgium, 2015.

[36] CEN, EN 1427:2015. Bitumen and bituminous binders – Determination of the softening point: Ring and Ball method, European Committee for Standardization, Brussels, Belgium, 2015.

[37] CEN, EN 13302: Bitumen and bituminous binders - Determination of dynamic viscosity of bituminous binder using a rotating spindle apparatus, European Committee for Standardization, Brussels, 2018.

[38] M. Cabette, R. Micaelo, J. Pais, Self-healing asphalt roads: evaluation of calcium alginate capsules with bio-oil, Transp. Res. Procedia 72 (2023) 688–695, https://doi.org/10.1016/j.trpro.2023.11.456.

[39] CEN, EN 933-10:2009. Tests for geometrical properties of aggregates. Part 10: Assessment of fines - Grading of filler aggregates (air jet sieving)., European Committee for Standardization, Brussels, 2009.

[40] ASTM, ASTM C 188-95 (reapproved 2003). Standard Test Method for Density of Hydraulic Cement., ASTM International, USA, 2003.

[41] IPQ, NP EN 1097-4:2012. Tests for mechanical and physical properties of aggregates – Part 4: Determination of the voids of dry compacted filler., Instituto Português da Qualidade, Caparica, 2012.

[42] C. Carl, P. Lopes, M. Sá da Costa, G. Canon Falla, S. Leischner, R. Micaelo, Comp. Study Eff. Long. -Term. Ageing Behav. Bitum. mastics Miner. Fill., Constr. Build. Mater. 225 (2019) 76–89, https://doi.org/10.1016/j.conbuildmat.2019.07.150.

[43] AASHTO, TP 101-14: Estimating Damage Tolerance of Asphalt Binders Using the Linear Amplitude Sweep, American Association of State Highway and Transportation Officials, Washington, D.C., 2014.

[44] C. Hintz, Understanding Mechanisms Leading to Asphalt Binder Fatigue, PhD Thesis, University of Wisconsin–Madison, 2012.

[45] F. Canestrari, A. Virgili, A. Graziani, A. Stimilli, Modeling and assessment of self-healing and thixotropy properties for modified binders, Int. J. Fatigue 70 (2015) 351–360, https://doi.org/10.1016/j.ijfatigue.2014.08.004.

[46] A. Stimilli, G. Ferrotti, C. Conti, G. Tosi, F. Canestrari, Chemical and rheological analysis of modified bitumens blended with "artificial reclaimed bitumen, Constr. Build. Mater. 63 (2014) 1–10, https://doi.org/10.1016/j.conbuildmat.2014.03.047.

[47] V. Antunes, A.C. Freire, L. Quaresma, R. Micaelo, Influence of the geometrical and physical properties of filler in the filler–bitumen interaction, Constr. Build. Mater. 76 (2015) 322–329, https://doi.org/10.1016/j.conbuildmat.2014.12.008.

[48] H. Bahia, H.A. Tabatabaee, T. Mandal, A. Faheem, Field Validation of Wisconsin Modified Binder Selection Guidelines - Phase II, University of Wisconsin-Madison, Modified Asphalt Research Center, Madison, USA, 2013.

[49] R. Micaelo, A. Pereira, L. Quaresma, M.T. Cidade, Fatigue resistance of asphalt binders: assessment of the analysis methods in strain-controlled tests, Constr. Build. Mater. 98 (2015) 703–712, https://doi.org/10.1016/j.conbuildmat.2015.08.070.

[50] H. Zhang, K. Shen, G. Xu, J. Tong, R. Wang, D. Cai, X. Chen, Fatigue resistance of aged asphalt binders: an investigation of different analytical methods in linear amplitude sweep test, Constr. Build. Mater. 241 (2020) 118099, https://doi.org/10.1016/j.conbuildmat.2020.118099.

[51] F. Safaei, C. Castorena, Y.R. Kim, Linking asphalt binder fatigue to asphalt mixture fatigue performance using viscoelastic continuum damage modeling, Mech. Time-Depend. Mater. 20 (2016) 299–323, https://doi.org/10.1007/s11043-016-9304-1.
[52] M. Cabette, R. Micaelo, J. Pais, Fatigue resistance of unaged and aged bio-bitumen: time sweep test versus linear amplitude sweep test, J. Test. Eval. 53 (2025), https://doi.org/10.1520/JTE20240213.
[53] G. Leegwater, A. Taboković, O. Baglieri, F. Hammoum, H. Baaj, Terms and Definitions on Crack-Healing and Restoration of Mechanical Properties in Bituminous Materials, in: H. Baaj, E. Chailleux, G. Tebaldi, C. Sauzéat, S. Mangiafico (Eds.), in: H. Di Benedetto, Proceedings of the RILEM International Symposium on Bituminous Materials, Springer International Publishing, Cham, 2022, pp. 47–53, https://doi.org/10.1007/978-3-030-46455-4_6.
[54] L.F. de A.L. Babadopulos, C. Sauzéat, H.D. Benedetto, Softening and local self-heating of bituminous mixtures during cyclic loading, Road. Mater. Pavement Des. 18 (2017) 164–177, https://doi.org/10.1080/14680629.2017.1304260.
[55] H.D. Benedetto, Q.T. Nguyen, C. Sauzéat, Nonlinearity, heating, fatigue and thixotropy during cyclic loading of asphalt mixtures, Road. Mater. Pavement Des. 12 (2011) 129–158, https://doi.org/10.1080/14680629.2011.9690356.
[56] L.F. de A.L. Babadopulos, G. Orozco, C. Sauzéat, H. Di Benedetto, Reversible phenomena and fatigue damage during cyclic loading and rest periods on bitumen, Int. J. Fatigue 124 (2019) 303–314, https://doi.org/10.1016/j.ijfatigue.2019.03.008.
[57] R. Varma, R. Balieu, N. Kringos, A state-of-the-art review on self-healing in asphalt materials: mechanical testing and analysis approaches, Constr. Build. Mater. 310 (2021) 125197, https://doi.org/10.1016/j.conbuildmat.2021.125197.
[58] X. Lu, U. Isacsson, Effect of ageing on bitumen chemistry and rheology, Constr. Build. Mater. 16 (2002) 15–22, https://doi.org/10.1016/S0950-0618(01)00033-2.
[59] G.D. Airey, Rheological evaluation of ethylene vinyl acetate polymer modified bitumens, Constr. Build. Mater. 16 (2002) 473–487, https://doi.org/10.1016/S0950-0618(02)00103-4.
[60] D. Lesueur, The colloidal structure of bitumen: consequences on the rheology and on the mechanisms of bitumen modification, Adv. Colloid Interface Sci. 145 (2009) 42–82, https://doi.org/10.1016/j.cis.2008.08.011.
[61] J. Petersen, A Review of the Fundamentals of Asphalt Oxidation. Chemical, Physicochemical, Physical Property, and Durability Relationships., Transportation Research Board, Washington, D.C, 2009.
[62] G. Sun, B. Li, D. Sun, J. Zhang, C. Wang, X. Zhu, Roles of aging and bio-oil regeneration on self-healing evolution behavior of asphalts within wide temperature range, J. Clean. Prod. 329 (2021) 129712, https://doi.org/10.1016/j.jclepro.2021.129712.
[63] E. Gaudenzi, F. Cardone, X. Lu, F. Canestrari, Analysis of fatigue and healing properties of conventional bitumen and bio-binder for road pavements, Materials 13 (2020), https://doi.org/10.3390/ma13020420.